Electronic Supporting Information

Propane dehydrogenation over extra-framework In(I) in chabazite zeolites

Yong Yuan and Raul F. Lobo*

Center for Catalytic Science and Technology, Department of Chemical and Biomolecular Engineering, University of Delaware, Newark, Delaware 19716, United States

*Email: lobo@udel.edu

Contents

S1. Experimental section……..S2

S2. Supporting tables and figures……..S7

Reference……..……...…S49

S1. Experimental section

1.1 Catalyst Preparation

Commercial H-CHA samples were obtained by calcining NH_4-CHA (ACS Material: SSZ-13 Zeolite, Type A) at 550 ℃ for 8 h in flowing air with a ramp rate of 2 ℃·min^{-1}. The Si/Al ratio of commercial H-CHA zeolite was determined to be 10.7 ± 1.1 by X-ray fluorescence (XRF, Rigaku WDXRF), which was referred to as H-CHA(11). The CHA zeolites with varying Si/Al ratios were synthesized using *N*,*N*,*N*-trimethyl-1-adamantanammonium ion ($TMAda^+$) as the structure-directing agent (SDA) based on protocols described in previous reports.[1,2] To prepare CHA zeolite with Si/Al ratio of 5, 20 g sodium silicate solution (Sigma-Aldrich, 26.5%) and 0.64 g sodium hydroxide (NaOH, Sigma-Aldrich, 99.99%) were added to 48 g de-ionized (DI) H_2O at room temperature and stirred for 15 min, followed by the addition of 2 g NH_4-Y zeolite (Zeolyst, CBV 500) and stirring for 30 min. Then, 8.4 g of TMAdaOH (SACHEM Inc., 25% aqueous solution) was added to the solution and stirred for another 30 min. The hydrothermal synthesis was carried out at 140 ℃ for 6 days under rotation. The zeolite samples were centrifuged at 4500 rpm for 10 min, washed with DI water 5 times, and dried at 80 ℃ overnight. The as-made zeolites were calcined in flowing air at 580 ℃ for 8 h with a ramp rate of 2 ℃·min^{-1} to remove the occluded $TMAda^+$. The calcined sample was referred to as Na-CHA(5). Afterward, Na-CHA(5) was ion-exchanged with 1M ammonium nitrate aqueous solution (NH_4NO_3, 99%, Sigma-Aldrich) at 80 ℃ for 3 h (1 g zeolite corresponds to 150 mL solution) and then centrifugated to remove the supernatant. This process was repeated three times, and then NH_4-CHA(5) was dried at 80 ℃ overnight and treated at 550 ℃ for 8 h in flowing air with a ramp rate of 2 ℃·min^{-1} to obtain H-CHA(5) samples. For the preparation of H-CHA(12), 13 g tetraethyl orthosilicate (TEOS, Sigma-Aldrich) was mixed with 26.4 g TMAdaOH and 2.264 g DI water at room temperature and stirred for 2 h, followed by the addition of 0.7 g aluminum ethoxide ($Al(OC_2H_5)_3$, Sigma-Aldrich) and stirred for an additional 1 h. The resulting solution was then hydrothermally at 150 ℃ for 6 days under static conditions. The produced crystals were centrifuged, washed, dried and calcined with the same procedure as the CHA(5) samples. The CHA zeolite with a Si/Al ratio of 25 was prepared using the same method as the H-CHA(12) except that the aluminum ethoxide content was decreased to 0.35 g. The Si/Al ratios of H-CHA(5), H-CHA(12), H-CHA(25) were measured by XRF and were determined to be 4.7 ± 0.3, 12.0 ± 1.3, and 24.8 ± 3.0, respectively.

Incipient wetness impregnation with an aqueous solution of indium (III) nitrate hydrate (Sigma-Aldrich) was used to prepare In-CHA samples with varying In/Al ratios. For example, for the preparation of In-CHA(11, 1.0) with In/Al ratio of 1.0, 0.58 g indium(III) nitrate hydrate was dissolved in 1.26 mL DI water. The prepared aqueous indium solution was added dropwise to 1 g H-CHA(11), followed by drying at 80 ℃ before calcining at 600 ℃ in flowing air for 2 h with a ramp rate of 5 ℃·min^{-1}. The calcined In-CHA catalysts were denoted as In-CHA(x, y), where x and y represent the Si/Al ratio and In/Al ratio, respectively. 10In/SiO_2 (10 wt% In), 10In/Al_2O_3 (10 wt% In) were prepared by the same method with SiO_2 (Sigma-Aldrich, silica gel davisil, grade 646) and γ-Al_2O_3 (Alfa Aesar, 99.97% metals basis), respectively. In_2O_3 was purchased from Sigma-Aldrich (99.99%

trace metals basis) and used as received. We prepared $PtSn/Al_2O_3$ catalyst (1%Pt and 2.6%Sn) using incipient wetness impregnation with an aqueous solution of $H_2PtCl_6 \cdot 6H_2O$ (Sigma-Aldrich) and $SnCl_2 \cdot 2H_2O$ (Sigma-Aldrich) on γ-Al_2O_3.[3]

1.2 Materials Characterization

Micropore volumes of the zeolite samples (Table S1) were determined by N_2 adsorption at -196 °C on a Micromeritics 3Flex system using the t-plot method. The specific surface area of SiO_2 and Al_2O_3 supported catalyst (Table S2) was determined by the BET method. All samples were degassed overnight at 350 ℃ before the adsorption measurements. Powder XRD measurements were conducted on a Bruker D8 diffractometer with Cu Kα radiation (40 kV, 40 mA) in the range of $2\theta = 4-50°$ with a step size of 0.04° and 0.5 s per step. The morphology of the samples was obtained using a scanning electron microscope (SEM, Auriga-60, ZEISS) after coating with a gold/palladium alloy. The bright-field transmission electron microscopy (TEM) images were obtained with a JEOL (JEM-2010F) transmission electron microscope equipped with a field emission gun emitter at 200 kV. The samples were ultrasonically dispersed in methanol, and then the suspension was dropped onto a carbon-coated copper grid. ^{27}Al and ^{29}Si solid-state magic angle spinning nuclear magnetic resonance (MAS-NMR) spectra were acquired on an 11.7 T Bruker Avance III NMR spectrometer with a 4 mm HX probe at spinning speeds of 12 and 10 kHz for ^{27}Al and ^{29}Si respectively. Direct excitation of ^{27}Al and ^{29}Si were performed with pulses of 1.0 (^{27}Al) or 3.5 (^{29}Si) μs. 75 kHz ^1H decoupling was applied during the acquisition.

Reduced catalysts for characterizations were obtained by reducing the calcined samples in a tube furnace with 10 vol% H_2 at 600 °C for 30 min with a ramp rate of 10 °C·min^{-1} and then cooling to room temperature before removing for storage. H_2 temperature-programmed reduction (H_2-TPR) profiles of the calcined catalysts were obtained using a Micromeritics AutoChem II 2920 equipped with a TCD detector. A sample of about 100 mg of the catalyst was pretreated in He flow (50 mL·min^{-1}) at 200 °C for 1 h and then cooled to 60 °C. The TPR measurement was conducted by heating the sample to 800 °C with a ramp rate of 10 °C·min^{-1} in a flow of 10 vol% H_2/Ar (50 mL·min^{-1}). The H_2 consumption was determined after calibration using CuO as standard. TGA was performed on a Discovery TGA instrument under air flow (100 mL·min^{-1}) with temperature ramping (10 °C·min^{-1}) to 800 °C.

Ethylamine temperature-programmed desorption (TPD) using the inhouse-built pulse reactor (described later) to determine the Brønsted acid sites (BASs) density of CHA zeolites.[4] Typically, 50 mg of the catalyst with a particle size range of 20−40 mesh was loaded into a quartz tube, and dehydrated at 550 °C for 30 min in the flow of 45 mL·min^{-1} N_2. Subsequently, samples were cooled to 150 °C, followed by the introduction of ethylamine (99%, Sigma-Aldrich), which was achieved by vaporization of liquid ethylamine through a 50 μm capillary tube into the N_2 stream (45 mL·min^{-1}). The ethylamine signal monitored via online mass spectrometry returns to the initial stage, indicating that the adsorption is saturated. Then the sample was purged with He at the same temperature (150 °C, 400 mL·min^{-1}) for 1 h and subsequently heated to 550 °C (10 °C·min^{-1}), during which effluent was monitored using the mass spectrometry. The following AMUs were used for analysis: 27 (C_2H_4), 28 (N_2), 30 ($C_2H_5NH_2$). The ethylene

concentration was calibrated by pulsing a fixed volume (0.67 mL) of ethylene into the reactor under He flow.

1.3 Transmission Fourier Transformed Infrared Studies

In situ Fourier transform infrared (FTIR) spectra were collected on an Agilent CARY 660 spectrometer equipped with an MCT detector. Catalysts are pressed into self-supporting wafers of about 20 mg and loaded into a custom-made sample holder for vertical alignment in the infrared beam using a customized in situ transmission cell equipped with KBr windows.[5] Typical spectra are the result of 128 coadded scans per spectrum at a spectral resolution of 2 cm^{-1}. Vacuum levels of <0.01 mTorr in the transmission cell were achieved by connecting to a vacuum manifold equipped with a mechanical pump and a diffusion pump. The transmission cell was heated by heating tapes controlled by a PID controller with the thermocouple close to the sample wafer. Before all experiments, the samples were dehydrated at 550 °C for 30 min under a vacuum to remove all adsorbed molecules. Chemicals such as H_2, D_2, D_2O, dry air were introduced into the transmission cell and corresponding pressure was controlled via the vacuum manifold.

In situ transmission FTIR with d_3-acetonitrile (CD_3CN) as probe molecule was employed to monitor the presence of BASs and Lewis acid sites (LASs).[6] The self-supporting wafer (~20 mg) was dehydrated at 550 °C for 30 min and then treated with H_2 (1 atm) at the same temperature. Introducing H_2 into the transmission cell three times for 10 min each time to ensure that the catalyst was completely reduced. The sample was then cooled to 50 °C under vacuum and then the excess of d_3-acetonitrile was introduced into the transmission cell followed by evacuation. The dosing procedure was repeated three times to ensure the complete saturation of the sample with d_3-acetonitrile. Next, the transmission cell was evacuated for 15 min to remove the physisorbed d_3-acetonitrile before collecting the spectrum.

1.4 Pulse Reactor Studies

An inhouse-built pulse reactor was used to determine the H_2/O_2 consumption of the catalyst at reaction temperature (Fig. S1).[7] Typically, two concurrent gas flows are controlled by calibrated mass flow controllers. An automatic 6-way valve (Vici) connected with a 0.67 mL loop and a 4-way valve are connected to provide pulses or continuous flow. A catalyst sample of 150 mg loaded into a silica glass tube (1/4 inch in diameter) is heated up to 600 °C at a ramp rate of 10 °C·min^{-1} in N_2 flow (45 mL·min^{-1}). A second gas stream, consisting of pure H_2 or pure O_2, flows through the loop. Once the sample temperature reaches the target temperature, the loop gas is pulsed via the bypass (Fig. S1) until a stable peak area is achieved, before introducing the periodic pulses into the reactor tube. The in-house instrument has a fast response time in that the pulse signal is detected in less than 10 seconds after switching the 6-way valve. The time interval between pulses is 30 min for H_2 pulses and 2 min for O_2 pulses. The catalyst can be reduced by 10 vol% H_2/N_2 or 10 vol% D_2/N_2 flow by switching the 4-way valve. The feed composition and product are analyzed by online mass spectrometry (Pfeiffer Omnistar). The following AMUs were used for analysis: 2 (H_2), 3 (HD), 4 (D_2), 18 (H_2O), 28(N_2), 32 (O_2). The quantification of

formed H_2O is determined by the calibration using CuO as standard (one mole CuO consumes one mole of H_2 and forms one mole of H_2O).

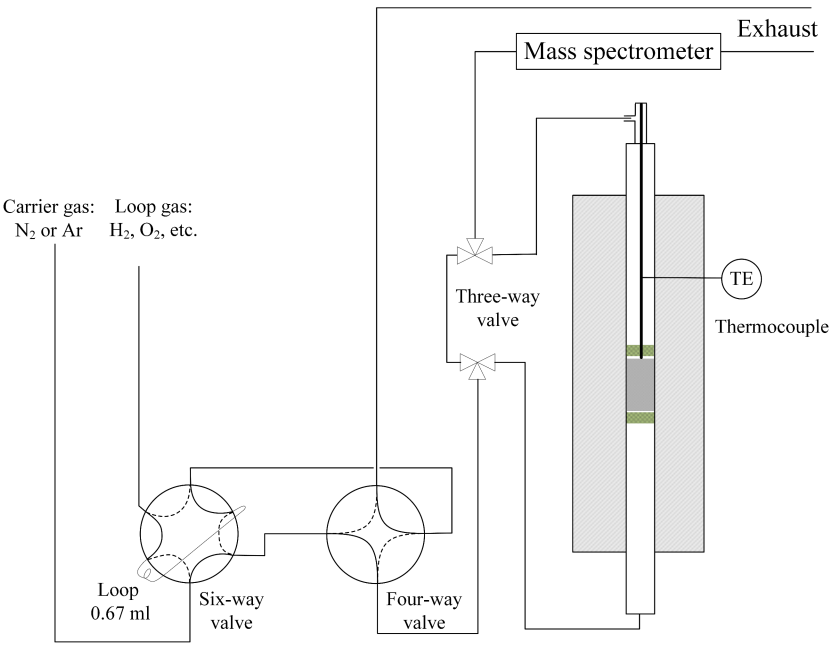

Fig. S1 Schematic of the pulse reactor.

1.5 Catalytic Reaction Rate Measurements

Catalytic reaction rates were measured using a fixed bed plug flow reactor, consisting of a quartz glass tube ($^1/_4$ inch in diameter). The catalyst bed typically contained 15—300 mg of the catalyst with a particle size range of 20−40 mesh. A thermocouple was placed close to the catalyst bed to ensure accurate temperature measurement. Before the rate measurements, the catalyst was heated to 600 °C for 30 min with a ramp rate of 10 °C·min^{-1} in 10 vol% H_2 with balancing N_2 (20 mL·min^{-1}), followed by purging with N_2 at the same temperature for another 30 min. The reduced sample was then exposed to 2.5 vol% C_3H_8 with balancing N_2 (total flow rate: 20 mL·min^{-1}) with the total pressure maintained at 101.32 kPa. The reactor effluent was periodically injected into an online gas chromatograph (GC) (Agilent 7890), using a heated gas line. The GC was equipped with an RT-Q-BOND column and flame ionization detector (FID) used for product analysis. FID response factors for CH_4, C_2H_4, C_3H_6, C_3H_8 were calibrated before the product analysis. The conversion of C_3H_8 was calculated using Eq. S1, the selectivity and yield of CH_4, C_2H_4, C_3H_6 were determined using Eqs. S2-S3.

$$\text{Conversion} = \left(1 - \frac{F_{C_3H_8,\,\text{outlet}}}{F_{C_3H_8,\,\text{inlet}}}\right) \times\ 100\% \tag{S1}$$

$$\text{Selectivity} = \frac{n_i \times F_{i,\,\text{outlet}}}{\sum n_i \times F_{i,\,\text{outlet}}} \times\ 100\% \tag{S2}$$

$$\text{Yield} = \frac{n_i \times F_{i,\,\text{outlet}}}{3 \times F_{C_3H_8,\,\text{inlet}}} \times\ 100\% \tag{S3}$$

$$\text{Carbon balance} = \frac{3 \times F_{C_3H_8,\,\text{outlet}} + \sum n_i \times F_{i,\,\text{outlet}}}{3 \times F_{C_3H_8,\,\text{inlet}}} \times 100\% \quad \text{(S4)}$$

where i represents the propane dehydrogenation products CH_4, C_2H_4, C_3H_6 in the effluent gas, n_i is the number of carbon atoms of component i, F_i is the molar flow rate. The C_3H_8 conversion was measured at differential conversions (< 6%) to avoid secondary reactions. PDH rates were determined from C_3H_6 yield, while C_3H_8 cracking rates were determined from the yields of CH_4 and C_2H_4. Apparent activation energies were determined in the temperature range of 580−620 °C. Carbon balance (Eq. S4) in rates measurement of In-based catalysts was higher than 97%.

The dependence of reaction rates on propane partial pressure for In-CHA(11, 1.0) was determined at 600 °C changing propane flow rate (0.5 – 20 mL·min^{-1}) diluted with N_2 flow at a constant total flow rate (100 mL·min^{-1}). The H_2 rate dependence was determined by changing the H_2 flow rate (1 – 20 mL·min^{-1}) with constant propane flow (5 mL·min^{-1}) and corresponding N_2 flow rates with total flow rate constant (100 mL·min^{-1}). During the measurements, the reactants were switched to 5 vol% C_3H_8/N_2 with 100 mL·min^{-1} total flow rate every 10 h to assess the effect of catalyst deactivation.

S2. Supporting tables and figures

Table S1. Textural properties of H-CHA and In-CHA samples investigated in this work.

Sample	Micropore volume[a] ($cm^3 \cdot g^{-1}$)	Micropore volume[b] corrected ($cm^3 \cdot g^{-1}$)
H-CHA(11)	0.247	0.247
In-CHA(11, 1.0)	0.213	0.256
In-CHA(11, 1.0) reduced	0.199	0.233
H-CHA(5)	0.272	0.272
In-CHA(5, 1.0)	0.171	0.242
In-CHA(5, 1.0) reduced	0.110	0.148
H-CHA(12)	0.292	0.292
In-CHA(12, 1.0)	0.224	0.271
In-CHA(12, 1.0) reduced	0.200	0.234
H-CHA(25)	0.277	0.277
In-CHA(25, 1.0)	0.275	0.301
In-CHA(25, 1.0) reduced	0.266	0.286

[a]Calculated with the *t*-plot method obtained from N_2 physisorption isotherms.
[b]Corrected micropore volume by subtracting the mass of indium species in the In-CHA samples by assuming In_2O_3 and In^+ sites are predominant in the calcined and reduced samples, respectively.

Table S2. Textural properties of In-containing samples and supports investigated in this work.

Sample	BET Surface Area ($m^2 \cdot g^{-1}$)	BET Surface Area[a] corrected ($m^2 \cdot g^{-1}$)
SiO_2	285	-
10In/SiO_2	250	284
10In/SiO_2 reduced	262	291
Al_2O_3	79	-
10In/Al_2O_3	60	68
10In/Al_2O_3 reduced	51	57

[a]Corrected BET surface area is determined by subtracting the mass of indium species by assuming In_2O_3 and In(0) sites are predominant in the calcined and reduced samples, respectively.

Table S3. Composition of the prepared In-based catalysts.

Sample	In/Al ratio[a]	In loading (%)[a]
In-CHA(11, 1.0)	1.04	14.2
In-CHA(12, y)		
	0.32	4.9
	0.70	10.8
	0.98	12.3
	1.74	19.5
In-CHA(5, 1.0)	0.98	21.3
In-CHA(25, 1.0)	0.95	6.2
10In/Al_2O_3	-	9.6
10In/SiO_2	-	9.9

[a]Determined by XRF.

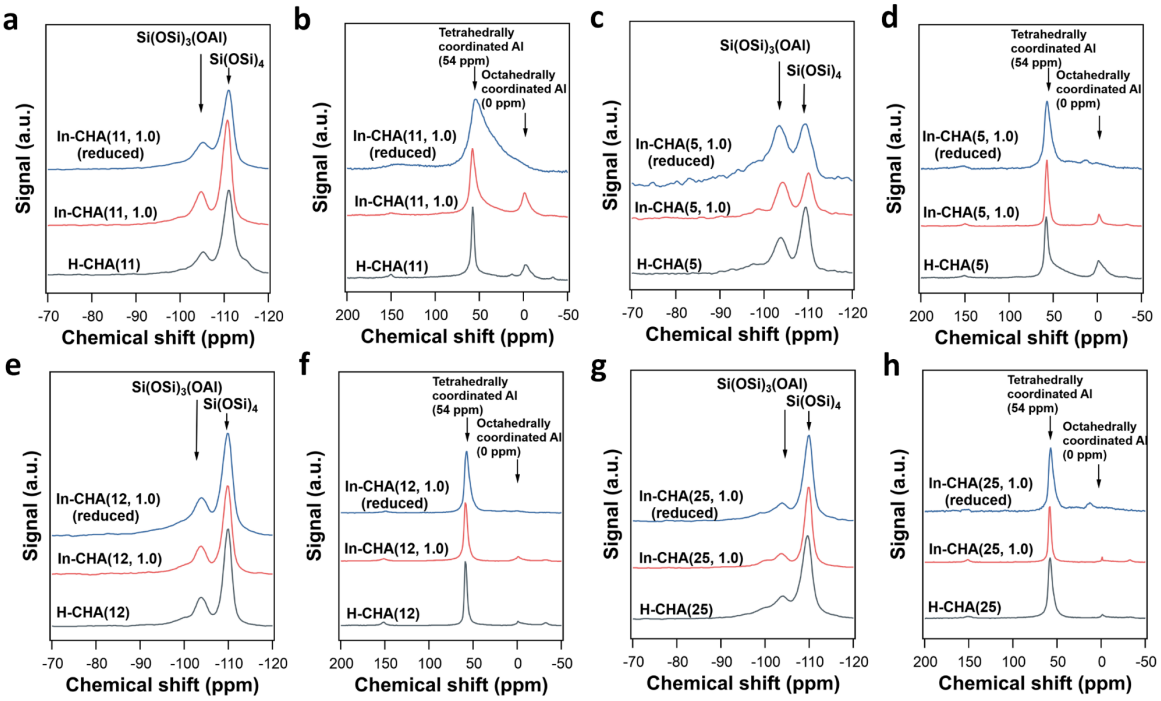

Fig. S2 Solid-state MAS-NMR spectra of the H-CHA and In-CHA with calcined and reduced conditions: (a, b) ^{29}Si NMR and ^{27}Al NMR of H-CHA(11) and In-CHA(11, 1.0); (c, d) ^{29}Si NMR and ^{27}Al NMR of H-CHA(5) and In-CHA(5, 1.0); (e, f) ^{29}Si NMR and ^{27}Al NMR of H-CHA(12) and In-CHA(12, 1.0); (g, h) ^{29}Si NMR and ^{27}Al NMR of H-CHA(25) and In-CHA(25, 1.0).

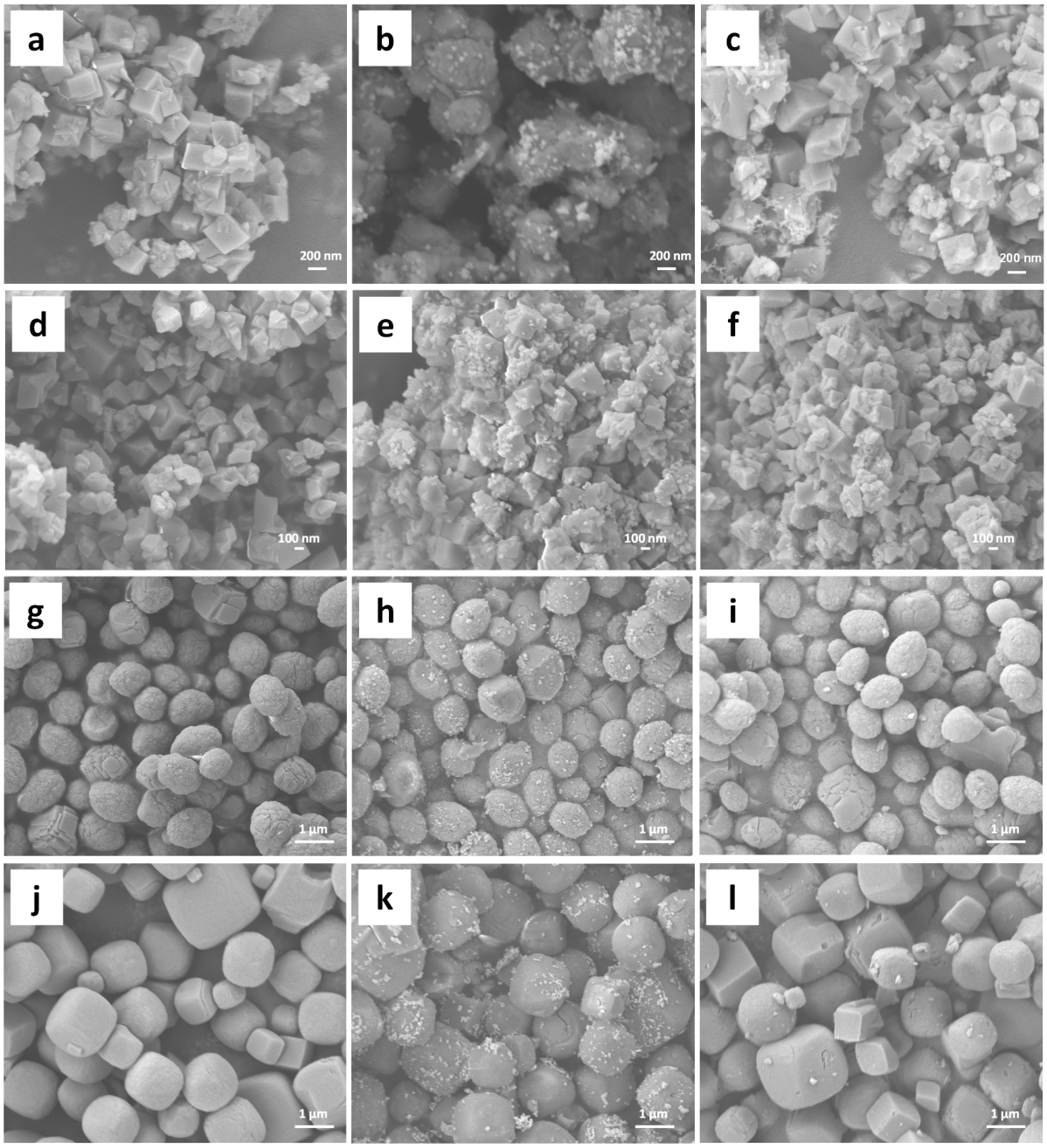

Fig. S3 SEM images of (a) H-CHA(11), (b) In-CHA(11, 1.0), (c) In-CHA(11, 1.0) reduced, (d) H-CHA(5), (e) In-CHA(5, 1.0), (f) In-CHA(5, 1.0) reduced, (g) H-CHA(12), (h) In-CHA(12, 1.0), (i) In-CHA(12, 1.0) reduced, (j) H-CHA(25), (k) In-CHA(25, 1.0), (l) In-CHA(25, 1.0) reduced samples.

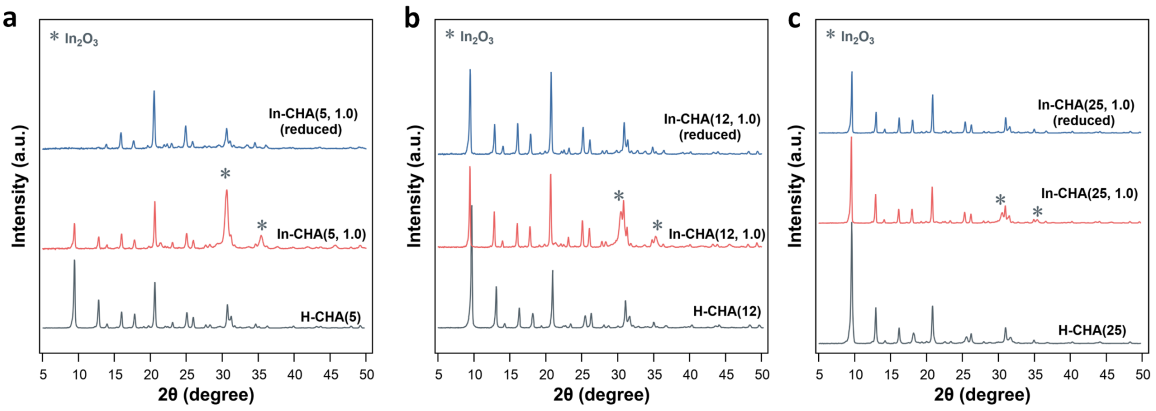

Fig. S4 XRD patterns of H-CHA(x) and In-CHA(x, 1.0) samples investigated after calcination and reduction: (a) x=5; (b) x= 12; (c) = 25. The diffraction peaks at 2θ values of 30.6°, 35.5° marked with asterisks are readily assignable to In_2O_3 (JCPDS 060416) on these catalysts.

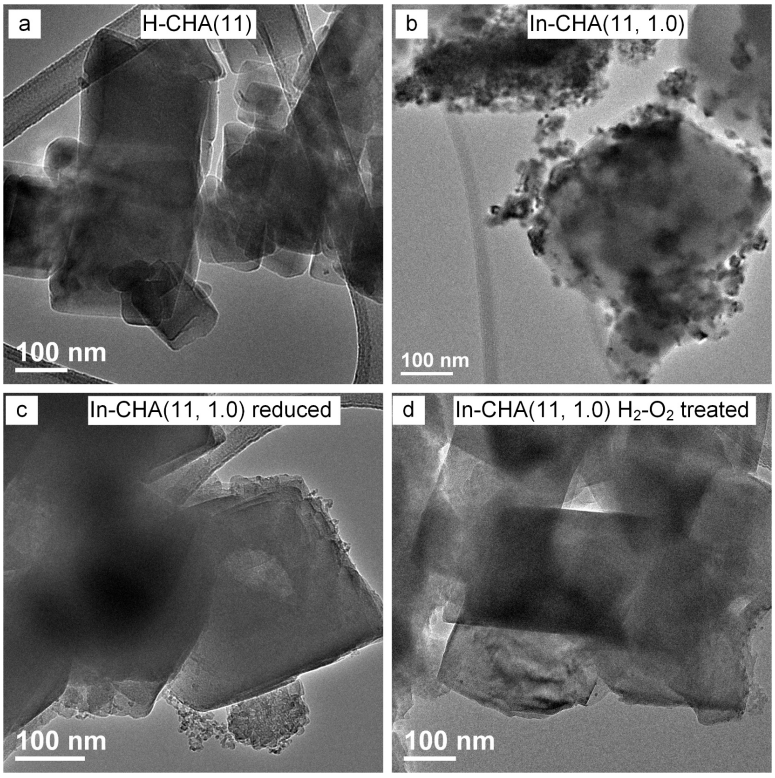

Fig. S5 TEM images of (a) H-CHA(11), (b) In-CHA(11, 1.0), (c) reduced In-CHA(11, 1.0), and (d) H_2-O_2 treated In-CHA(11, 1.0).

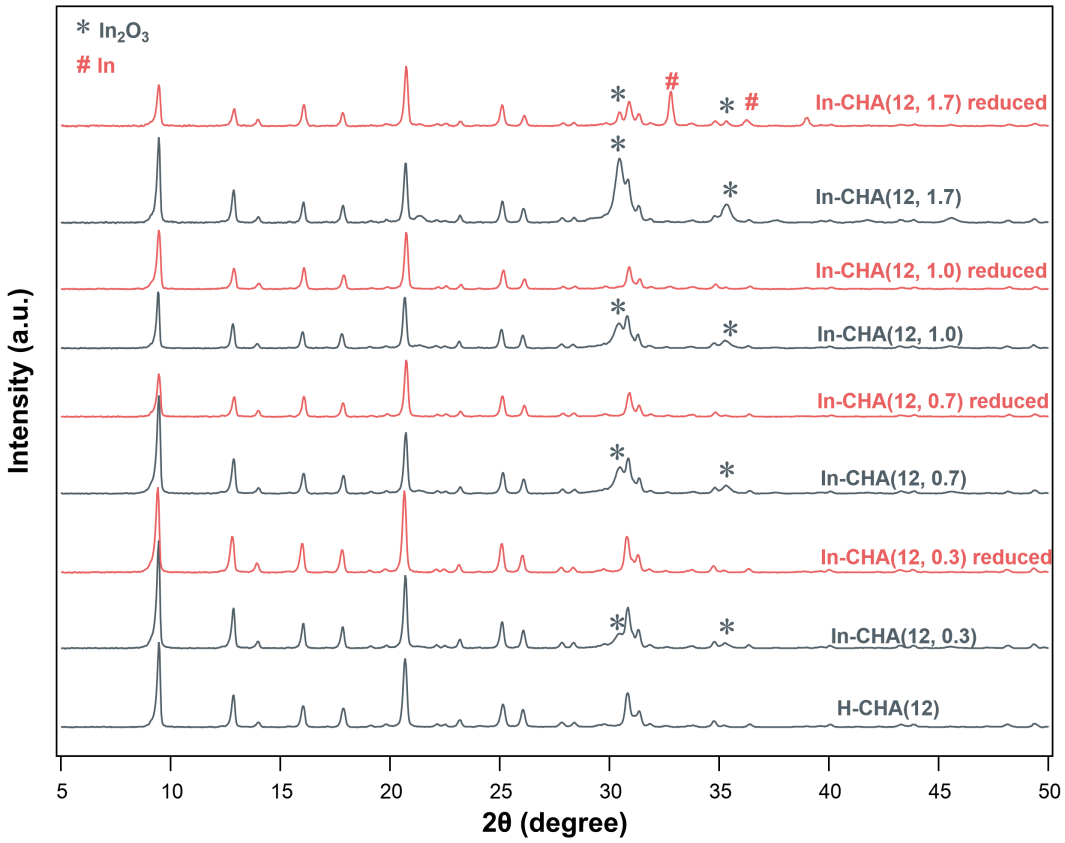

Fig. S6 XRD patterns of the In-CHA(12, y) samples with varying In/Al ratios from 0.3 to 1.7 (calcined and reduced conditions). The diffraction peaks at 2θ values of 30.6°, 35.5° marked with asterisks are assigned to In_2O_3 (JCPDS 060416), and diffraction peaks at 2θ values of 33.0°, 36.3° and 39.2° marked with # symbol are assigned to metallic In(0) (JCPDS 05-0642).

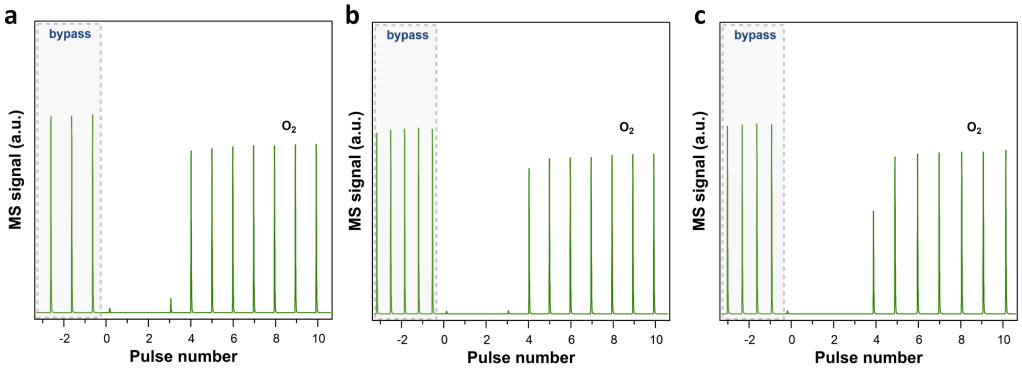

Fig. S7 O_2 pulses results on the In-CHA(11, 1.0) catalyst at 600 °C: (a) reduced by H_2 pulses on the calcined sample; (b) reduced by H_2 pulses on H_2-O_2 treated sample; (c) reduced by 10 vol% H_2 flow for 30 min.

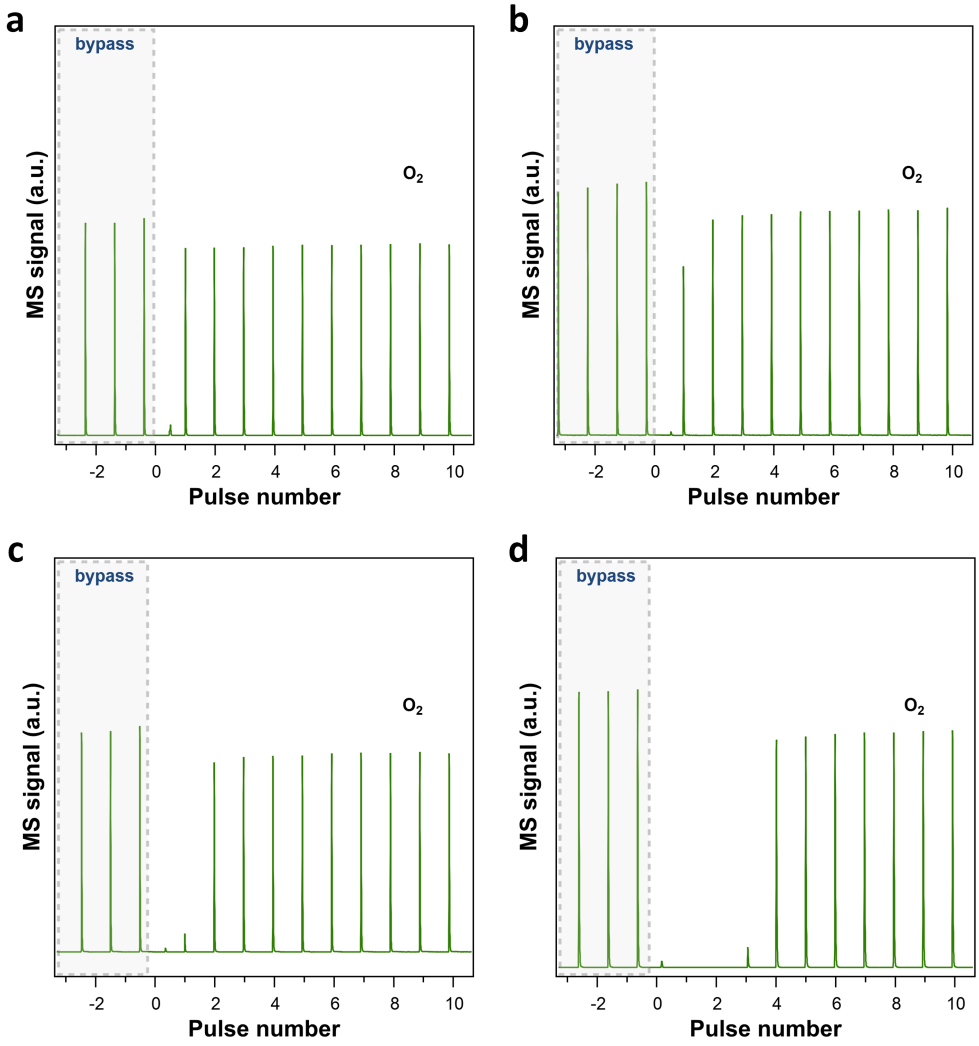

Fig. S8 O_2 pulses results on the In-based catalyst (reduced via H_2 pulses) at 600 °C: (a) In_2O_3; (b) $10In/SiO_2$; (c) $10In/Al_2O_3$; (d) In-CHA(11, 1.0).

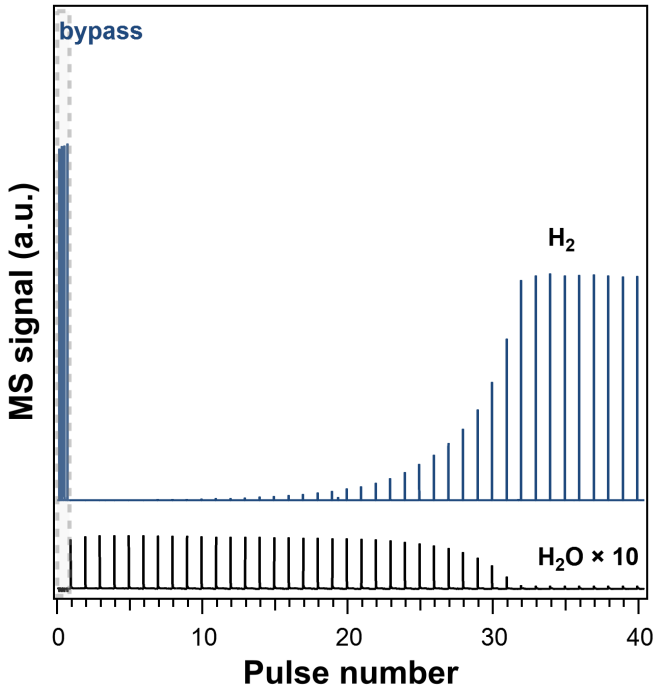

Fig. S9 H_2 pulses results of CuO catalyst for calibration of H_2O formation amounts. Test condition: 50 mg CuO, 600 °C. Cu: 625 μmol, consumed H_2: 655 μmol, formed H_2O: 640 μmol. H_2/Cu = 1.05 and H_2O/H_2= 0.98.

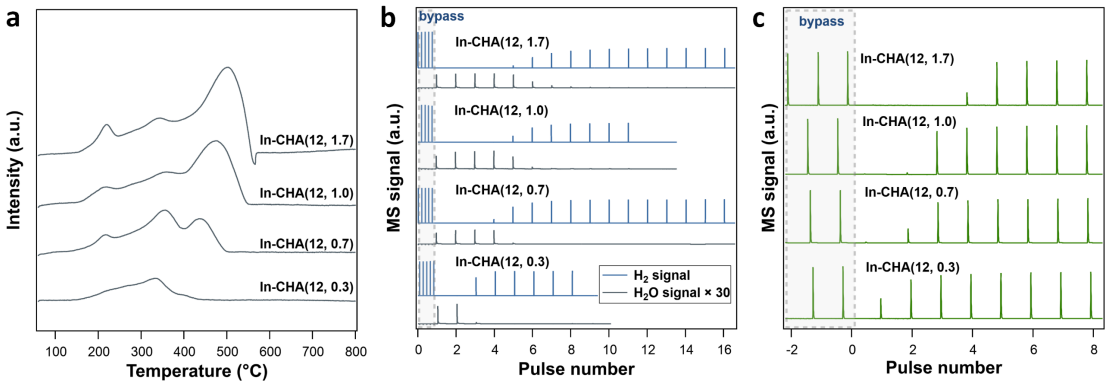

Fig. S10 (a) H_2-TPR profiles, (b) results of H_2 pulses experiments and (c) subsequent O_2 pulses at 600 °C on In-CHA(12, y) with varying In/Al ratios (as indicated in the figure legends).

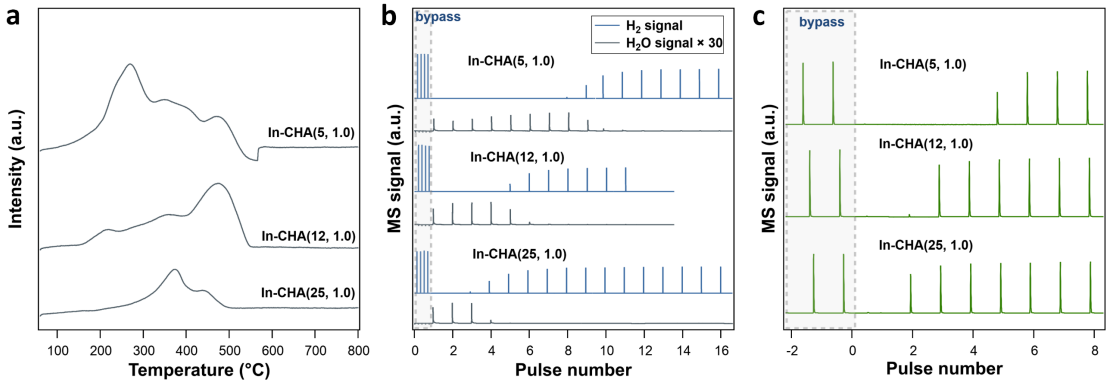

Fig. S11 (a) H_2-TPR profiles, (b) results of H_2 pulse experiments and (c) subsequent O_2 pulse at 600 °C on In-CHA(x, 1.0) with varying Si/Al ratios (as indicated in the figure legends).

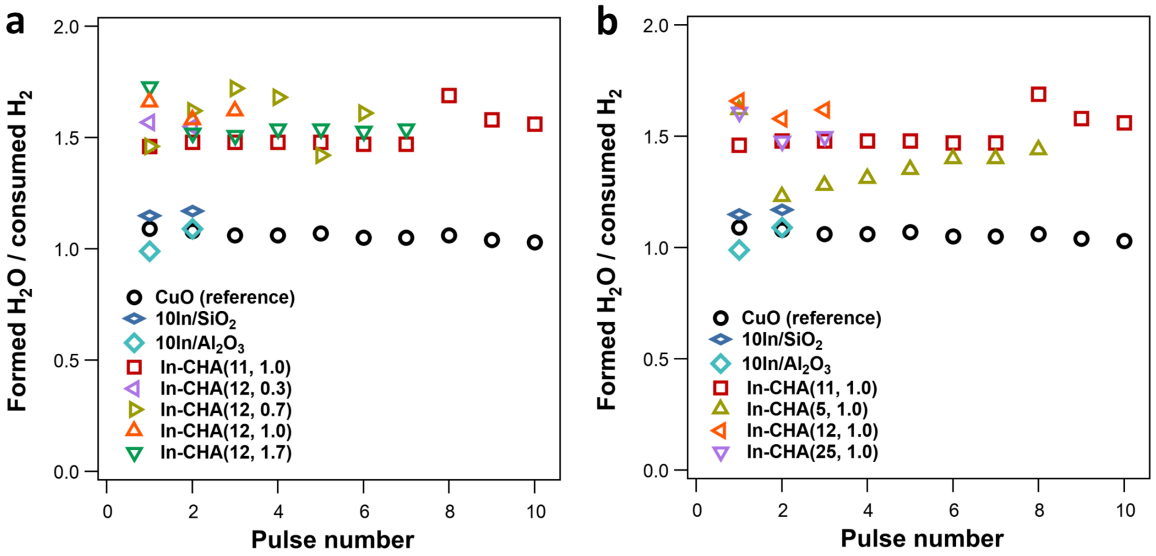

Fig. S12 Determination of formed H_2O/consumed H_2 ratio from H_2 pulses as a function of pulse number on varying catalysts: (a) In-CHA(12, y) with varying In/Al ratios and (b) In-CHA(x, 1.0) with varying Si/Al ratios.

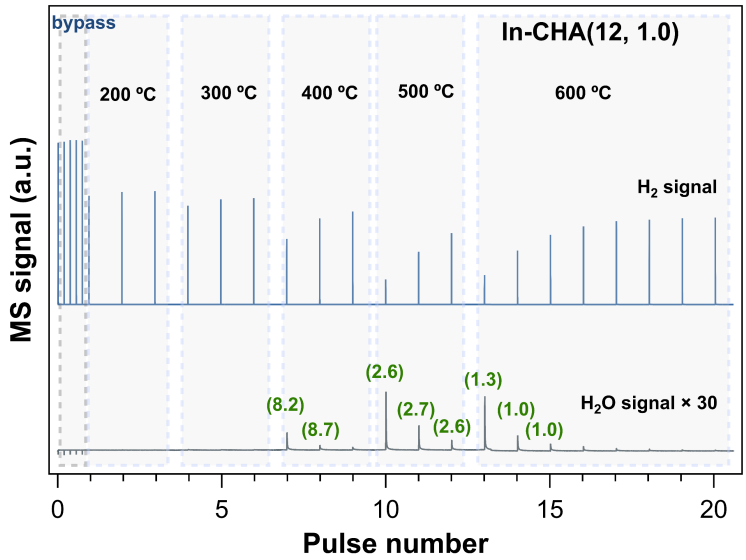

Fig. S13 Results of H_2 pulse experiments on In-CHA(12, 1.0) at different temperatures (as indicated in the figure). The number in parentheses represents the ratio of formed H_2O to consumed H_2 at a specific pulse.

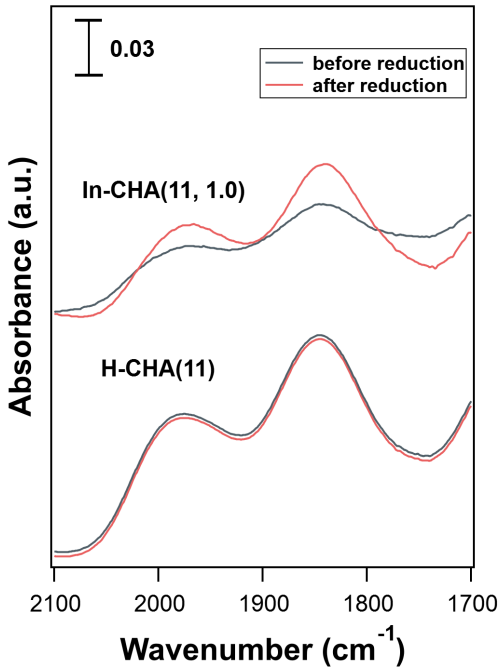

Fig. S14 FTIR spectra of In-CHA(11, 1.0) catalyst and H-CHA(11) catalyst collected during the H_2 reduction process at 550 °C (indicated in the figure legends). Black and red traces represent spectra before and after reduction by H_2 (1 atm) at 550 °C, respectively. The background spectrum was collected in the spectral cell without a sample pellet at room temperature under vacuum.

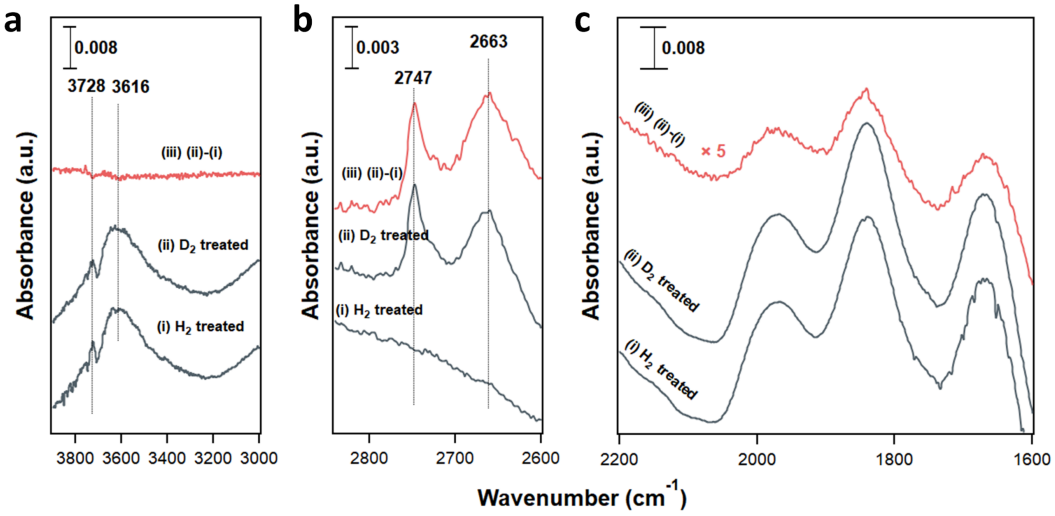

Fig. S15 FTIR spectra of reduced In-CHA(11, 1.0) catalyst at 550 °C in (a) high and (b, c) low wavenumber ranges: (i) after H_2 treatment; (ii) after D_2 treatment for 10 min; (iii) (i) subtracted from spectrum (ii). The background spectrum was collected in the spectral cell without a sample pellet at room temperature under vacuum.

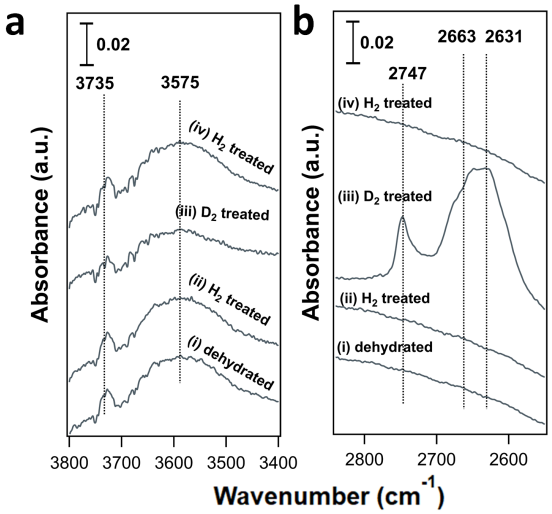

Fig. S16 FTIR spectra of H-CHA(11) catalyst at 550 °C in (a) high and (b) low wavenumber ranges: (i) after dehydration; (ii) after H_2 treatment for 10 min; (ii) after D_2 treatment for 10 min; (iv) after H_2 treatment for 10 min again. The background spectrum was collected in the spectral cell without a sample pellet at room temperature under vacuum.

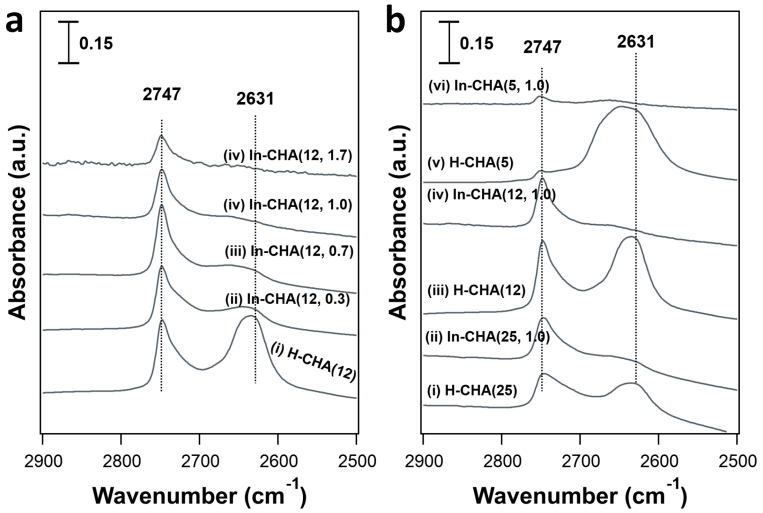

Fig. S17 FTIR spectra of D_2 reduced (a) In-CHA(12, y) with varying In/Al ratios ranging from 0 to 1.7 and (b) H-CHA(x, 1.0) with varying Si/Al ratios ranging from 5 to 25 catalysts at 550 °C (indicated in the figure legends). The background spectrum was collected in the spectral cell without a sample pellet at room temperature under vacuum.

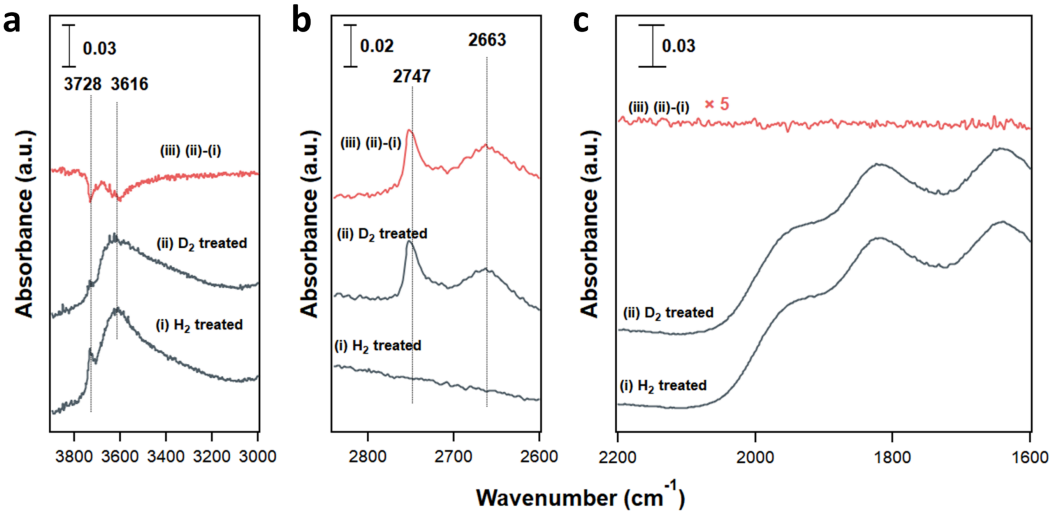

Fig. S18 FTIR spectra of reduced In-CHA(5, 1.0) catalyst at 550 °C in (a) high and (b, c) low wavenumber ranges: (i) after H_2 treatment; (ii) after D_2 treatment for 10 min; (iii) (i) subtracted from spectrum (ii). The background spectrum was collected in the spectral cell without a sample pellet at room temperature under vacuum.

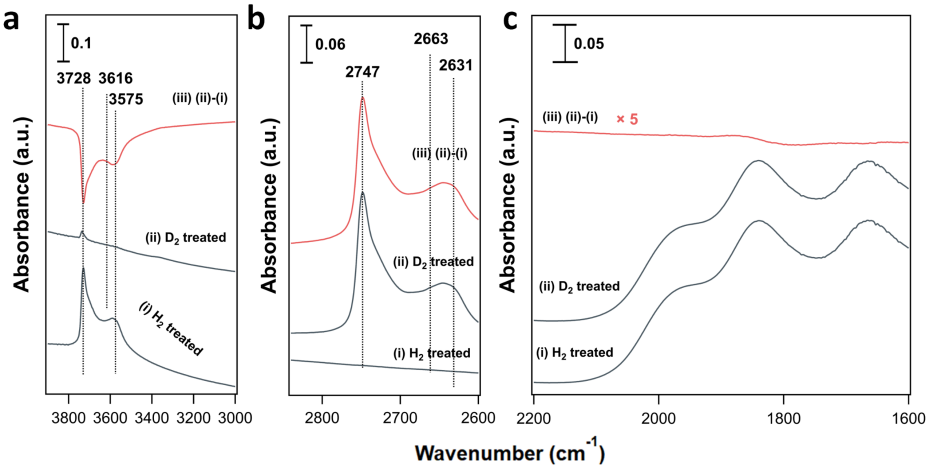

Fig. S19 FTIR spectra of reduced In-CHA(12, 0.3) catalyst at 550 °C in (a) high and (b, c) low wavenumber ranges: (i) after H_2 treatment; (ii) after D_2 treatment for 10 min; (iii) (i) subtracted from spectrum (ii). The background spectrum was collected in the spectral cell without a sample pellet at room temperature under vacuum.

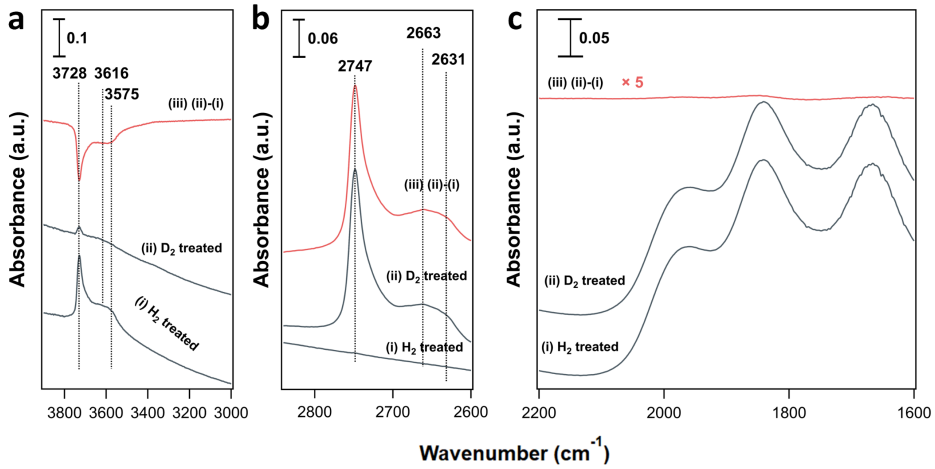

Fig. S20 FTIR spectra of reduced In-CHA(12, 0.7) catalyst at 550 °C in (a) high and (b, c) low wavenumber ranges: (i) after H_2 treatment; (ii) after D_2 treatment for 10 min; (iii) (i) subtracted from spectrum (ii). The background spectrum was collected in the spectral cell without a sample pellet at room temperature under vacuum.

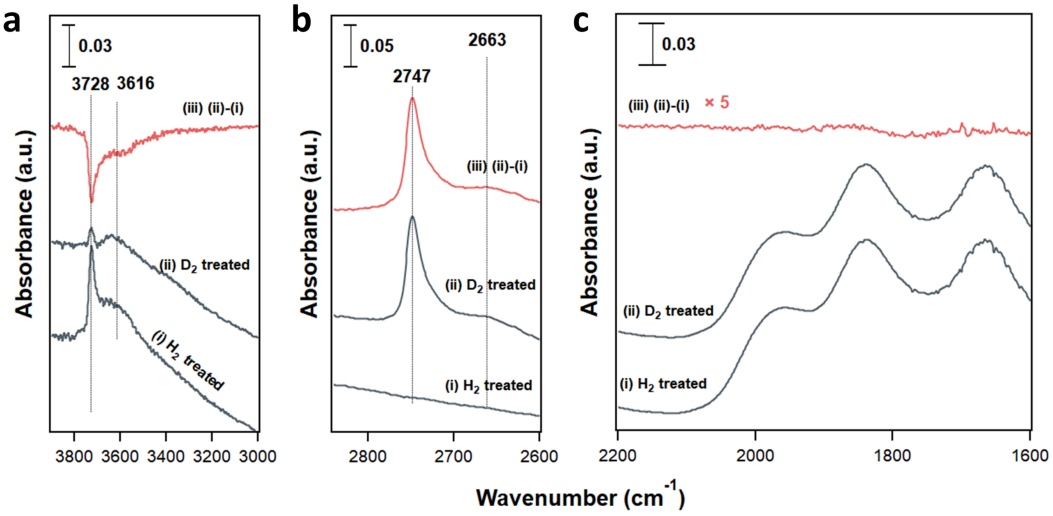

Fig. S21 FTIR spectra of reduced In-CHA(12, 1.0) catalyst at 550 °C in (a) high and (b, c) low wavenumber ranges: (i) after H_2 treatment; (ii) after D_2 treatment for 10 min; (iii) (i) subtracted from spectrum (ii). The background spectrum was collected in the spectral cell without a sample pellet at room temperature under vacuum.

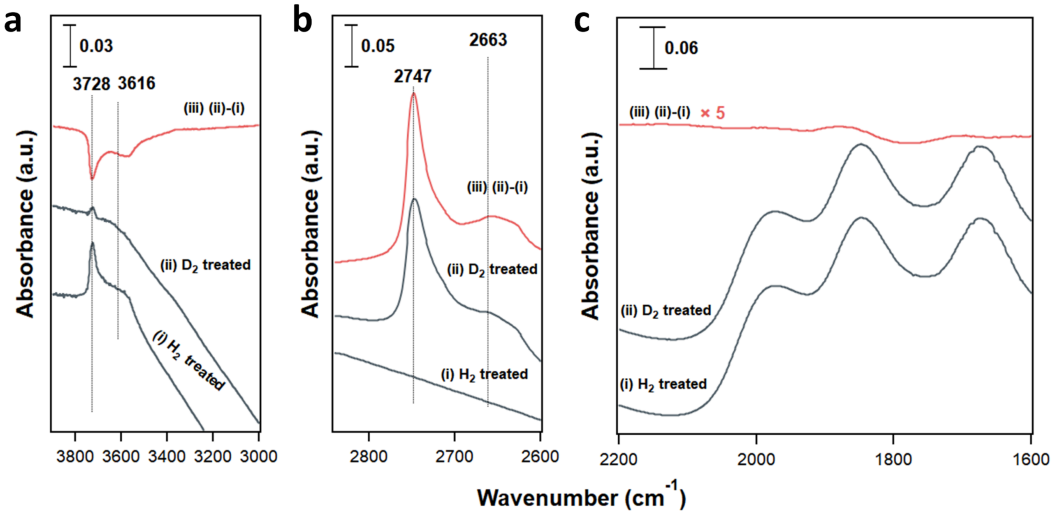

Fig. S22 FTIR spectra of reduced In-CHA(25, 1.0) catalyst at 550 °C in (a) high and (b, c) low wavenumber ranges: (i) after H_2 treatment; (ii) after D_2 treatment for 10 min; (iii) (i) subtracted from spectrum (ii). The background spectrum was collected in the spectral cell without a sample pellet at room temperature under vacuum.

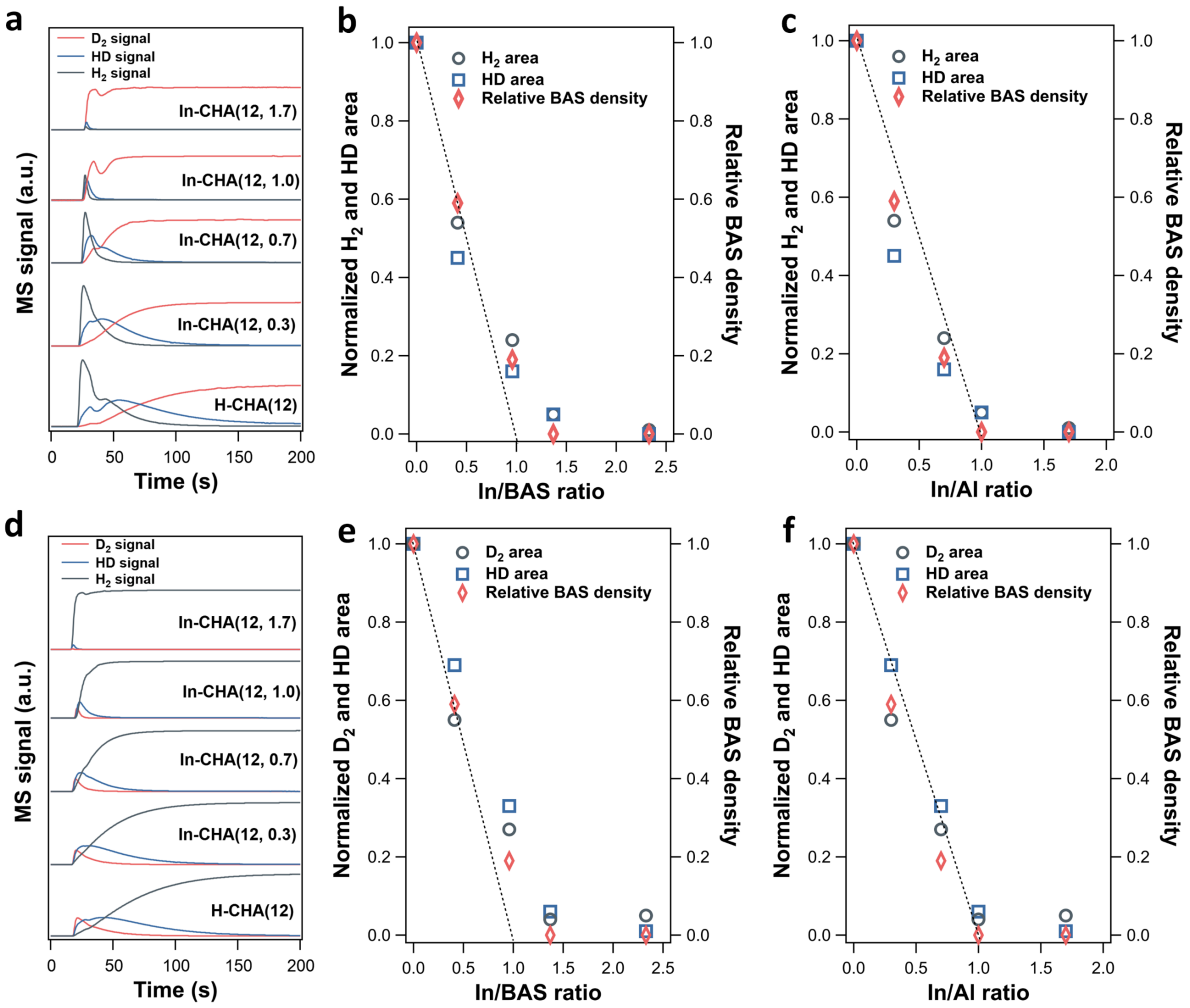

Fig. S23 (a) H_2 (2 amu), HD (3 amu), and D_2 (4 amu) signals as a function of time when switching the N_2 flow to 10 vol% D_2 flow on In-CHA(12, y) with In/Al ratios ranging from 0 to 1.7 (indicated in the figure legends). The samples were reduced via 10 vol% H_2/N_2 flow for 30 min and purged by N_2 flow for another 30min before switching to 10 vol% D_2 flow. (b, c) Integrated H_2 and HD peak area in (a) and relative BAS densities as a function of (b) In/BAS ratios and (c) In/Al ratios (normalized to the H_2 and HD peak area or BAS density of H-CHA(12)). (d) H_2, HD and D_2 signals as a function of time when switching the N_2 flow to 10 vol% H_2 flow on In-CHA(12, y) with varying In/Al ratios ranging from 0 to 1.7 (indicated in the figure legends). The samples were reduced via 10 vol% D_2/N_2 flow for 30 min and purged by N_2 flow for another 30min before switching to 10 vol% H_2 flow. (e, f) Integrated D_2 and HD peak area in (d) as a function of (e) In/BAS ratios and (f) In/Al ratios (normalized to the D_2 and HD peak area or BAS density of H-CHA(12)).

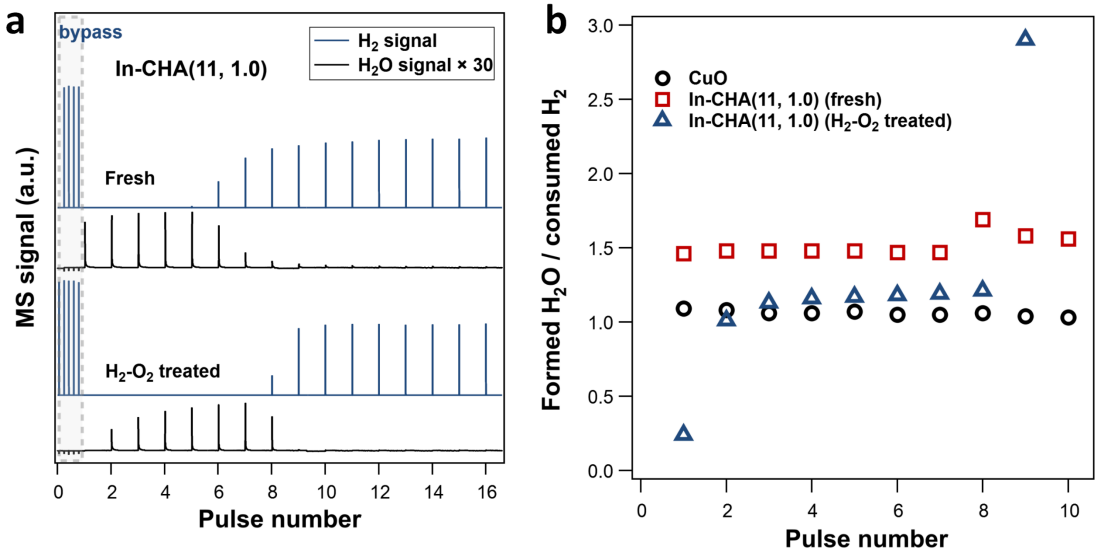

Fig. S24 (a) H_2 pulses results of In-CHA(11, 1.0) catalyst with calcined and H_2-O_2 treated conditions at 600 °C. (b) Determination of formed H_2O/consumed H_2 ratio from H_2 pulses as a function of pulse number on In-CHA(11, 1.0) catalyst with calcined and H_2-O_2 treated conditions.

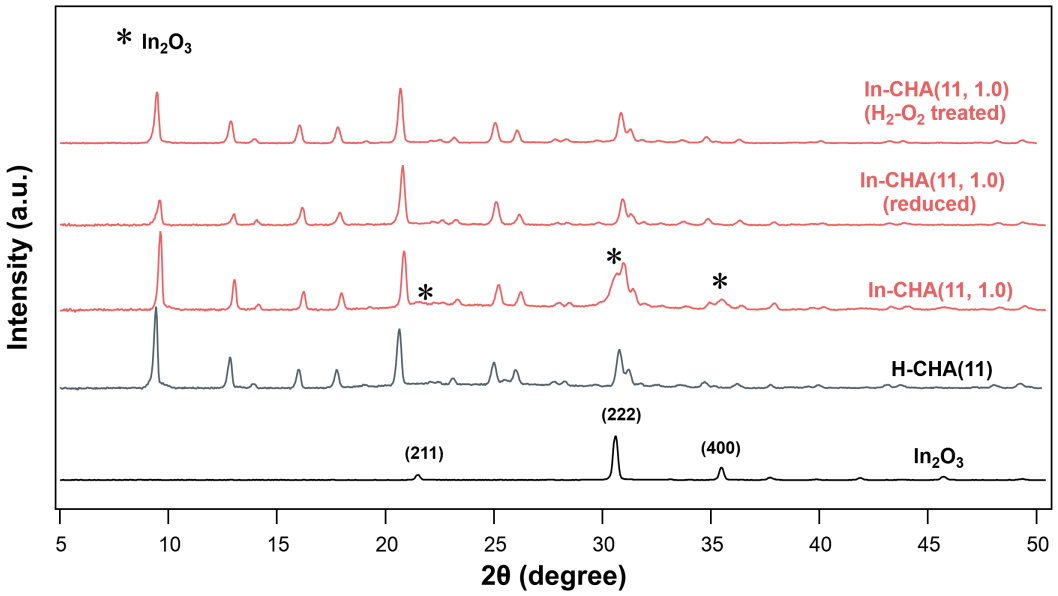

Fig. S25 XRD patterns of the H-CHA(11) and In-CHA(11, 1.0) samples with different treatments. The diffraction peaks at 2θ values of 30.6°, 35.5° marked with asterisks(*) are assigned to In_2O_3 (JCPDS 060416) on these catalysts.

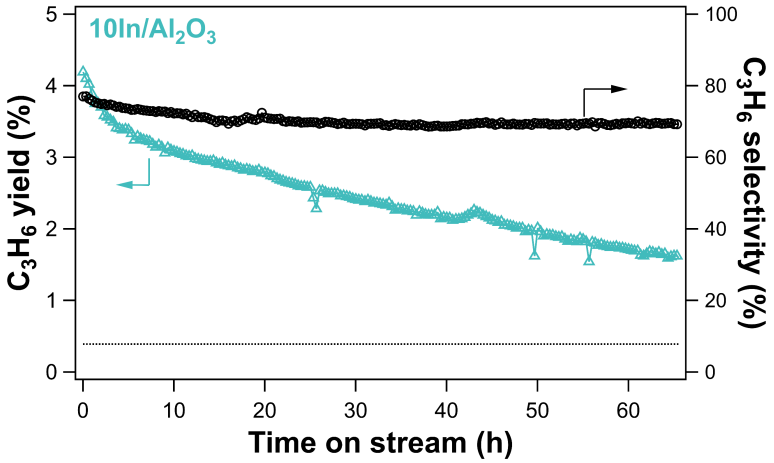

Fig. S26 C_3H_6 yield and C_3H_6 selectivity as a function of time on stream over $10In/Al_2O_3$. Reaction conditions: 600 °C, C_3H_8 partial pressure 2.54 kPa with balancing N_2, space time 806400 $g_{Cat}\cdot s\cdot mol_{C3H8}^{-1}$. The propane conversions are below 6% in the rate measurements. The dotted line in the figure represents the C_3H_6 yield without catalyst under the same conditions.

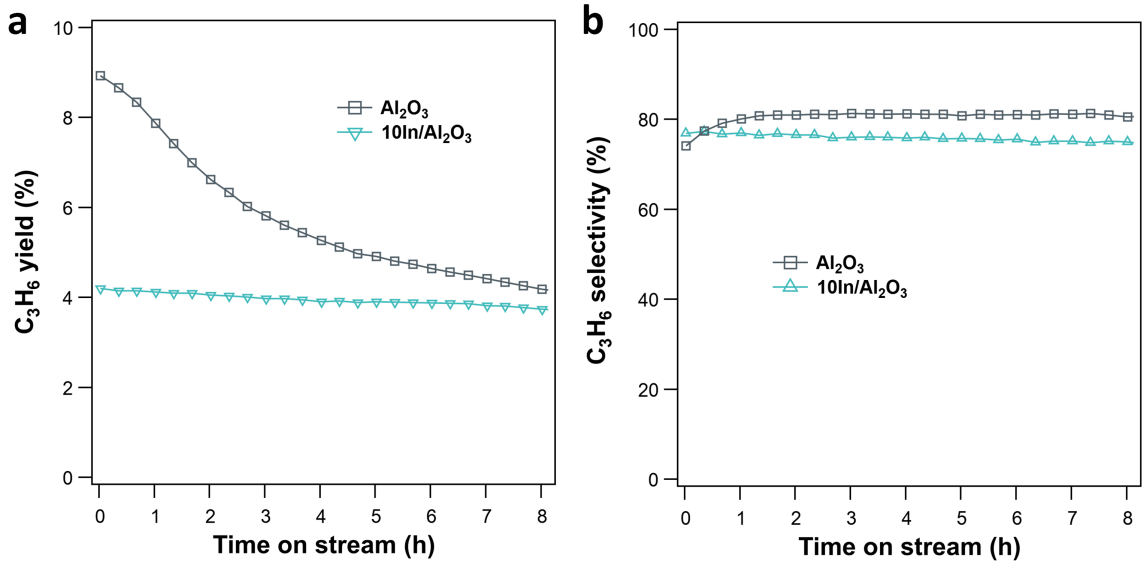

Fig. S27 (a) C_3H_6 yield and (b) C_3H_6 selectivity as a function of time on stream over 10In/Al_2O_3 and bare Al_2O_3 catalysts. Reaction conditions: 600 °C; C_3H_8 partial pressure, 2.54 kPa with balancing N_2, space time, 806400 $g_{Cat}{\cdot}s{\cdot}mol_{C3H8}^{-1}$.

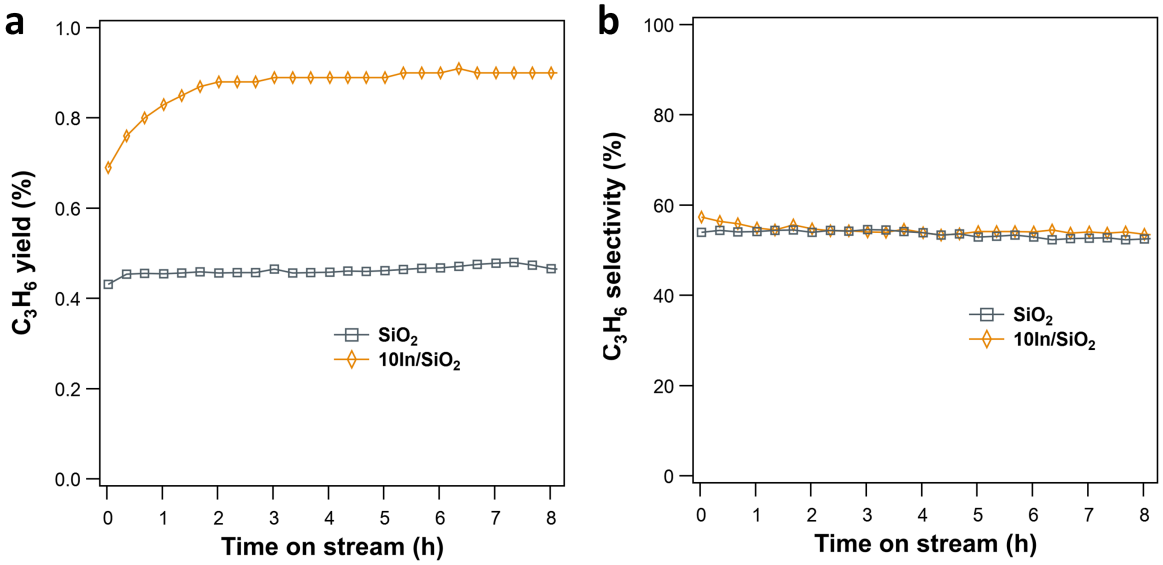

Fig. S28 (a) C_3H_6 yield and (b) C_3H_6 selectivity as a function of time on stream over 10In/SiO_2 and bare SiO_2 catalysts. Reaction conditions: 600 °C; C_3H_8 partial pressure, 2.54 kPa with balancing N_2, space time, 806400 $g_{Cat}\cdot s\cdot mol_{C3H8}^{-1}$.

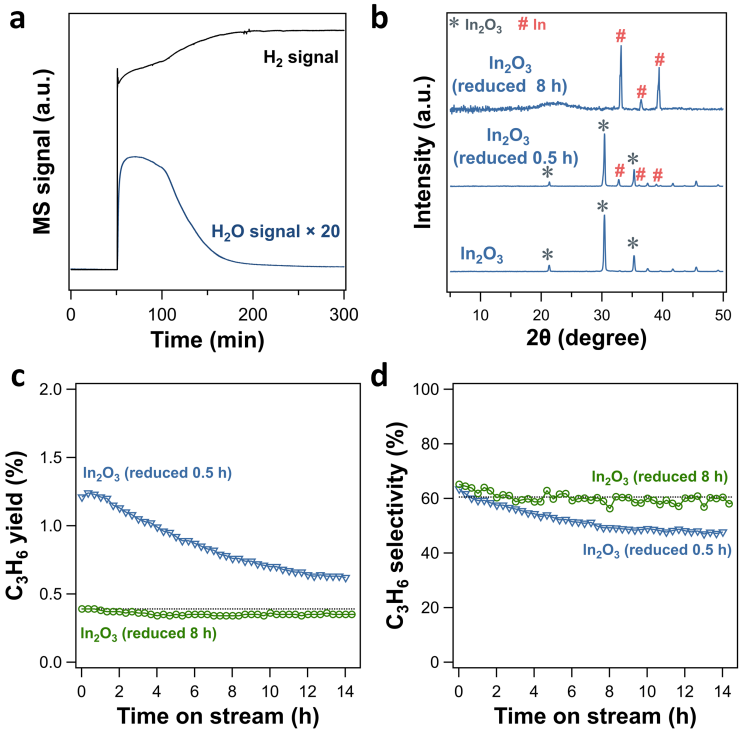

Fig. S29 (a) H_2O and H_2 signal during the in situ reduction of In_2O_3 at 600 °C. (b) XRD patterns of bulk In_2O_3 and reduced In_2O_3 with varying time. (c) C_3H_6 yield and (d) C_3H_6 selectivity as a function of time on stream over In_2O_3 with different reduction time. Reaction conditions: 600 °C, C_3H_8 partial pressure 2.54 kPa with balancing N_2, space time 806400 $g_{Cat}\cdot s\cdot mol_{C3H8}^{-1}$. The dotted line in the figure represents the C_3H_6 yield (0.39%) and C_3H_6 selectivity (60%) without catalyst under the same conditions.

Note: H_2-TPR profile of bulk In_2O_3 sample (Fig. 1a) shows that a higher reduction temperature is needed to bulk In_2O_3 sample than other samples such as In-CHA. Considering that H_2 pulses cannot reduce the bulk In_2O_3, we used 10 vol%H_2 flow to reduce the sample and monitored the formation of H_2O (Fig. S29a). The H_2O signal shows that a long time (~4 hours) is needed to completely reduce bulk the In_2O_3 at 600 °C, and the H_2O/In ratio was determined to be 1, suggesting that the In_2O_3 can be completely reduced to In(0). XRD pattern of reduced In_2O_3 sample (8 hours of reduction) shows no presence of bulk In_2O_3, but strong diffraction peaks of In(0), supporting the complete reduction of In_2O_3 to In(0), shown in Fig. S29b. Propane dehydrogenation tests show that In(0) is almost inactive for propane dehydrogenation (Fig. S29c and d). The gradually decreased reaction rates on the In_2O_3 sample (reduced 0.5 h) were interpreted as the gradual reduction of remaining In_2O_3 to In(0).

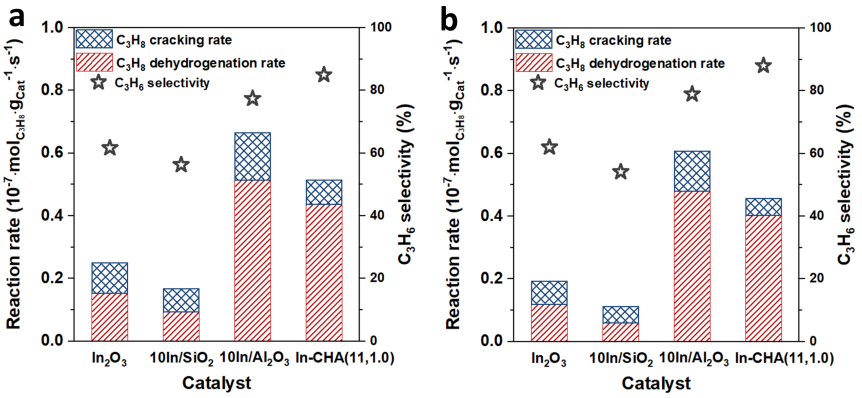

Fig. S30 (a) The reaction rates and C_3H_6 selectivity on the In-based catalyst. (b) The corrected reaction rates and C_3H_6 selectivity on In-based catalyst by subtracting the reaction rate derived from thermal cracking.

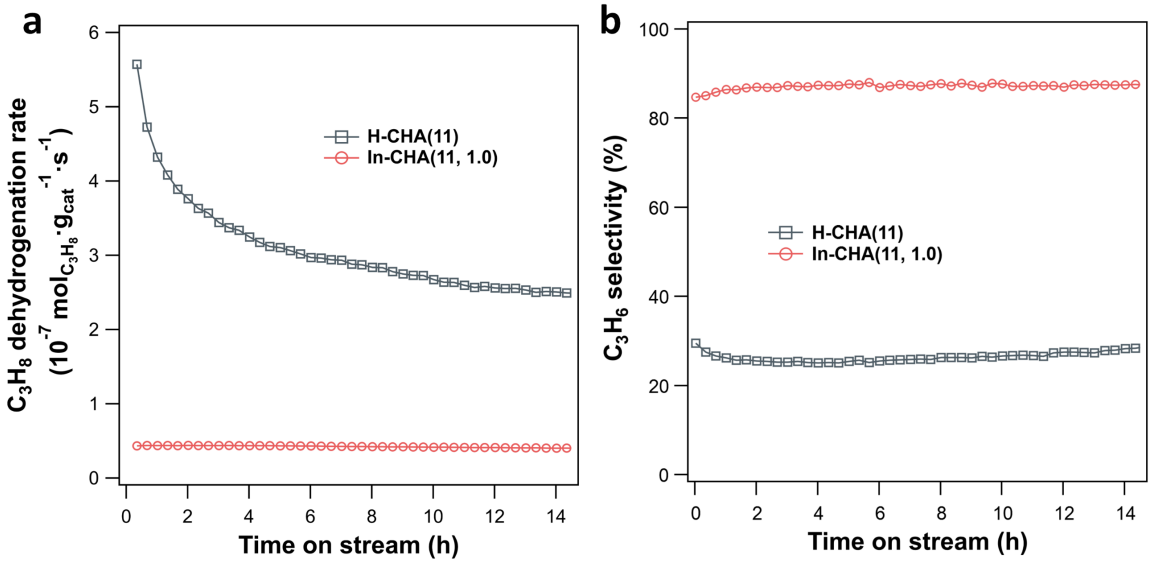

Fig. S31 (a) propane dehydrogenation rate and (b) C_3H_6 selectivity as a function of time on stream over H-CHA(11) and In-CHA(11, 1.0) catalysts. Reaction conditions: 600 °C; C_3H_8 partial pressure, 2.54 kPa with balancing N_2. The propane conversions are below 6% in the rate measurements.

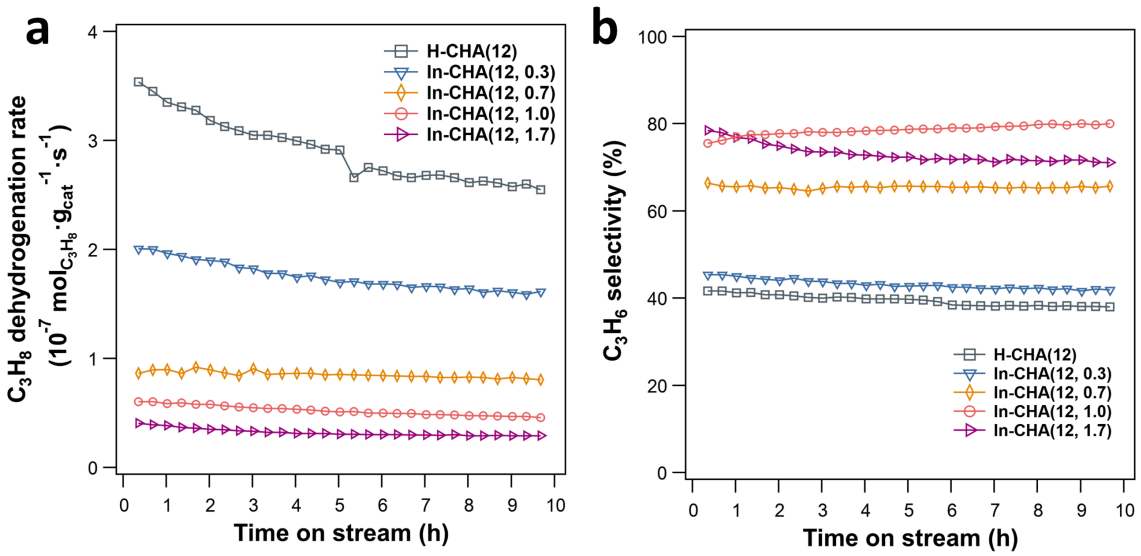

Fig. S32 (a) Propane dehydrogenation rate and (b) C_3H_6 selectivity as a function of time on stream over In-CHA(12, y) with varying In/Al ratios. Reaction conditions: 600 °C; C_3H_8 partial pressure, 2.54 kPa with balancing N_2. The propane conversion is below 6% in the rate measurements.

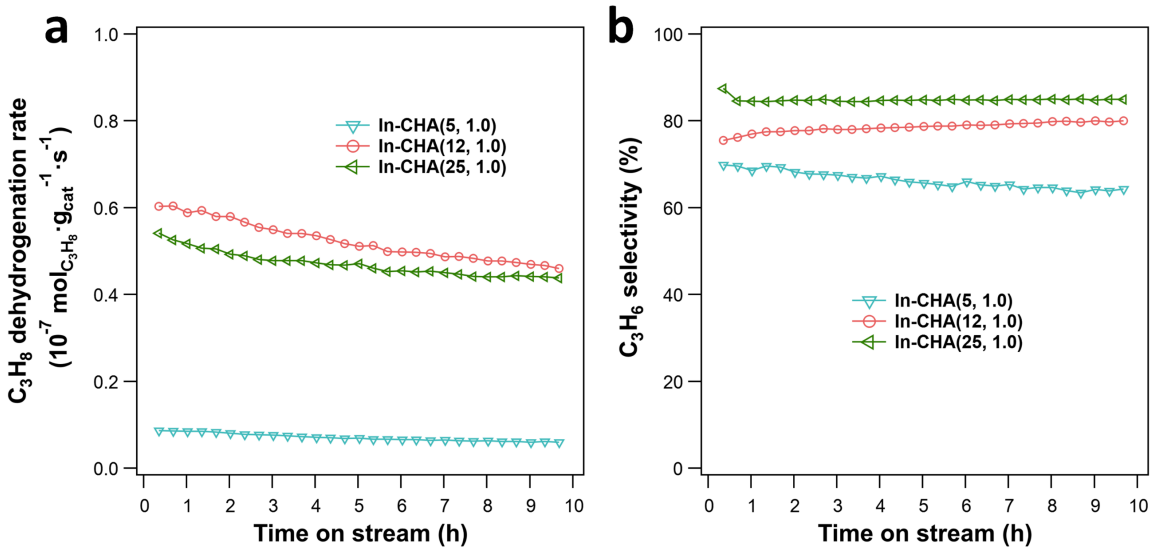

Fig. S33 (a) Propane dehydrogenation rate and (b) C_3H_6 selectivity as a function of time on stream over In-CHA(x, 1.0) with varying Si/Al ratios. Reaction conditions: 600 °C; C_3H_8 partial pressure, 2.54 kPa with balancing N_2. The propane conversion is below 6% in the rate measurements.

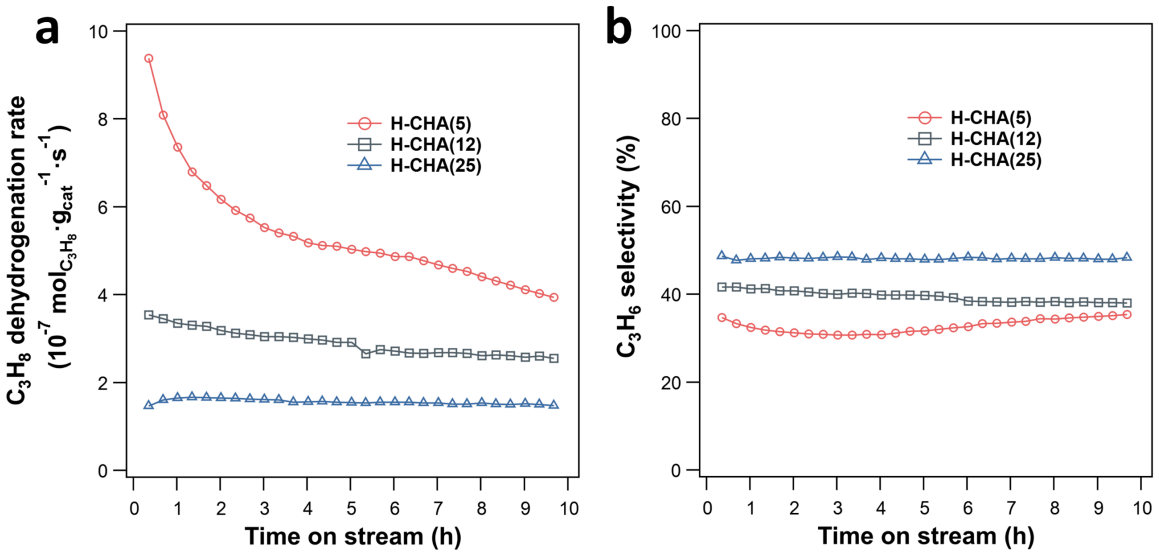

Fig. S34 (a) Propane dehydrogenation rate and (b) C_3H_6 selectivity as a function of time on stream over H-CHA(x) with varying Si/Al ratios. Reaction conditions: 600 °C; C_3H_8 partial pressure, 2.54 kPa with balancing N_2. The propane conversion is below 6% in the rate measurements.

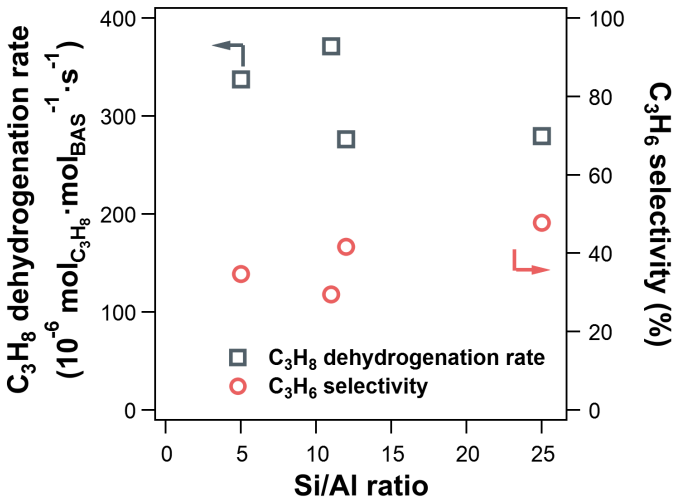

Fig. S35 C_3H_8 dehydrogenation rate and C_3H_6 selectivity as a function of Si/Al ratios on H-CHA catalysts investigated. Reaction rates were collected at TOS = 21 min. Reaction conditions: 600 °C; C_3H_8 partial pressure, 2.54 kPa with balancing N_2. The propane conversion is below 6% in the rate measurements.

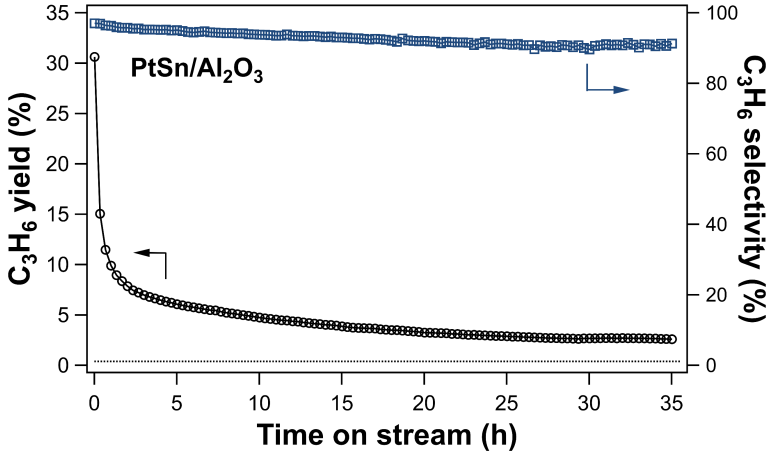

Fig. S36 C_3H_6 yield and C_3H_6 selectivity as a function of time on stream over $PtSn/Al_2O_3$. Reaction conditions: 600 °C, C_3H_8 partial pressure 2.54 kPa with balancing N_2, space time 134400 $g_{Cat}\cdot s\cdot mol_{C3H8}^{-1}$. The dotted line in the figure represents the C_3H_6 yield (0.39%) without catalyst under the same conditions.

Table S4. Values of turn-over frequency (TOF) and pre-exponential factor and entropy changes to propane dehydrogenation over In-CHA catalyst at 600 °C.

	TOF ($mol_{C3H8} \cdot mol_{In} \cdot s^{-1}$)	Apparent rate constant ($mol_{C3H8} \cdot mol_{In} \cdot s^{-1} \cdot bar^{-1}$)	Pre-exponential factor ($mol_{C3H8} \cdot mol_{In} \cdot s^{-1} \cdot bar^{-1}$)	ΔS^{app} ($J \cdot mol^{-1} \cdot K^{-1}$)
In-CHA(11, 1.0)	4.1×10^{-5}	1.5×10^{-3}	716	-207
In-CHA(25, 1.0)	8.8×10^{-5}	3.5×10^{-3}	11606	-184
In-CHA(12, 1.0)	5.2×10^{-5}	2.1×10^{-3}	6849	-189
In-CHA(5, 1.0)	2.7×10^{-5}	3.1×10^{-3}	47944839	-115

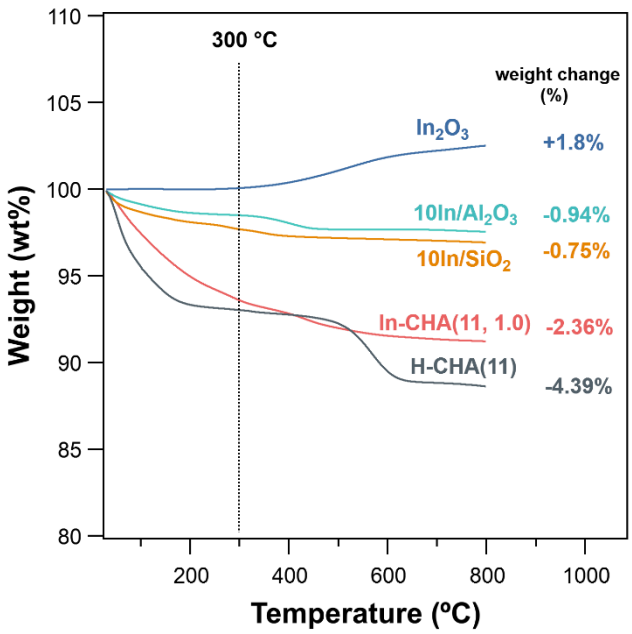

Fig. S37 TGA data of spent In-based catalyst. The catalysts were tested for 15 h reaction at 600 °C, C_3H_8 partial pressure was 2.54 kPa with balancing N_2.

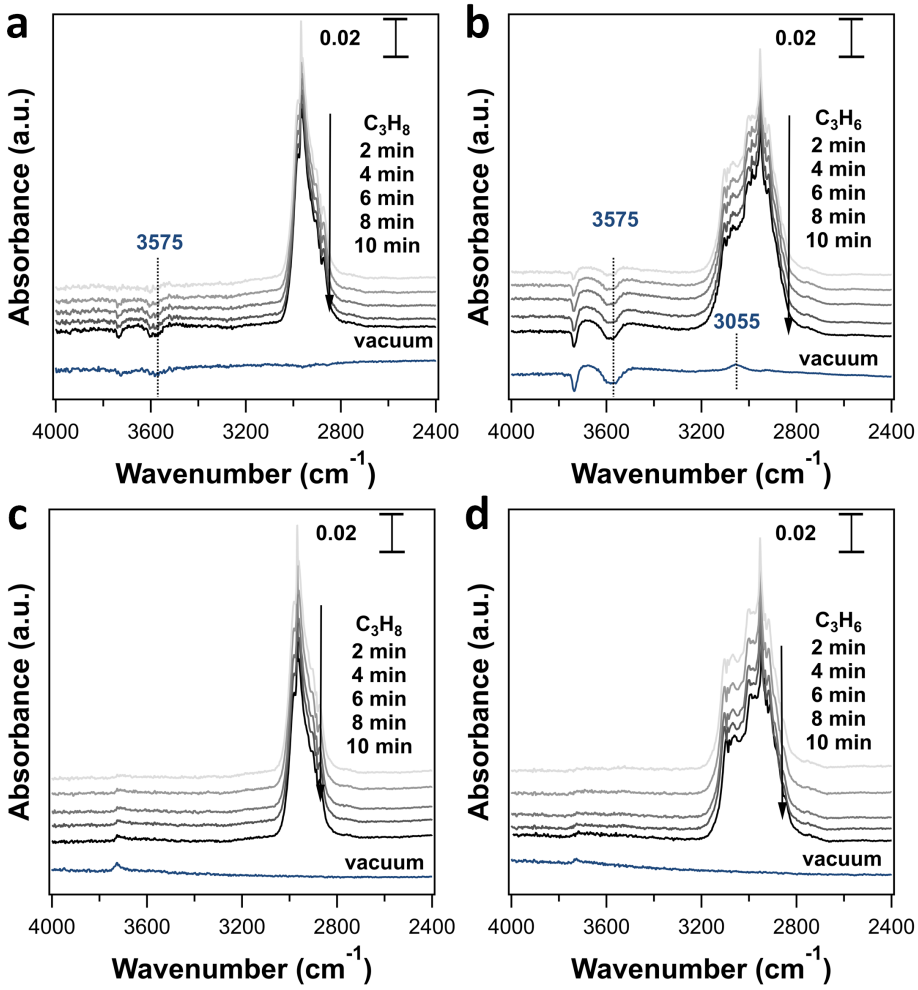

Fig. S38 (a, b) FTIR spectra of (a) C_3H_8 treatment (1.33 kPa) and (b) C_3H_6 treatment (1.33 kPa) on reduced H-CHA(12) for 2 min, 4 min, 6 min, 8 min, 10 min, respectively and after evacuation. (c, d) FTIR spectra of (a) C_3H_8 treatment (1.33 kPa) and (b) C_3H_6 treatment (1.33 kPa) on reduced In-CHA(12, 1.0) for 2 min, 4 min, 6 min, 8 min, 10 min, respectively and after evacuation. The background spectrum is collected in the spectral cell with a reduced sample pellet at 550 °C under vacuum.

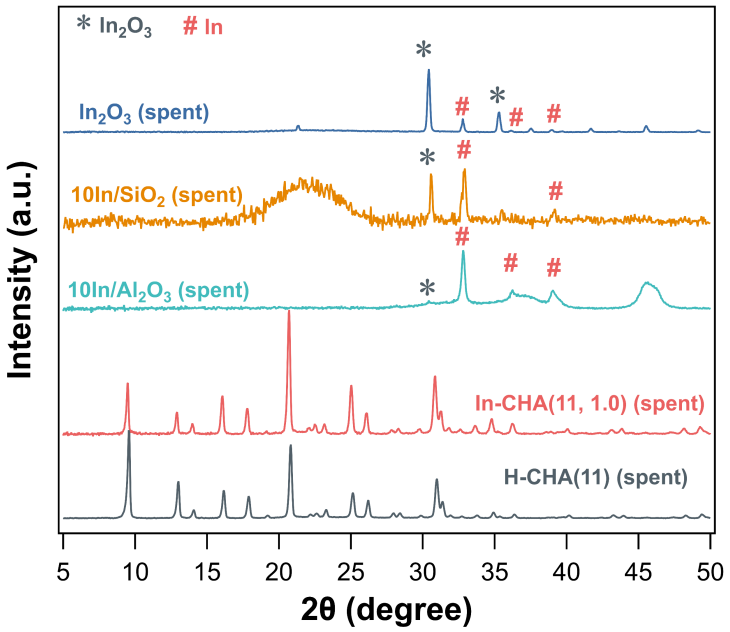

Fig. S39 XRD patterns of the spent catalyst. The diffraction peaks at 2θ values of 30.6°, 35.5° marked with asterisks are readily assignable to In_2O_3 (JCPDS 060416), and diffraction peaks at 2θ values of 33.0°, 36.3° and 39.2° marked with pound keys are associated with In(0) (JCPDS 05-0642) on these catalysts.

References

1. J. H. Yun and R. F. Lobo, *Catal. Sci. Technol.*, 2015, **5**, 264–273.
2. B. Ipek, M. J. Wulfers, H. Kim, F. Göltl, I. Hermans, J. P. Smith, K. S. Booksh, C. M. Brown and R. F. Lobo, *ACS Catal.*, 2017, **7**, 4291–4303.
3. A. H. Motagamwala, R. Almallahi, J. Wortman, V. O. Igenegbai and S. Linic, *Science*, 2021, **373**, 217–222.
4. J. E. Romo, T. Wu, X. Huang, J. Lucero, J. L. Irwin, J. Q. Bond, M. A. Carreon and S. G. Wettstein, *ACS Omega*, 2018, **3**, 16253–16259.
5. Y. Yuan, C. Brady, L. Annamalai, R. F. Lobo and B. Xu, *J. Catal.*, 2021, **393**, 60–69.
6. H. J. Cho, D. Kim and B. Xu, *ACS Catal.*, 2020, **10**, 4770–4779.
7. C. Brady, B. Murphy and B. Xu, *ACS Catal.*, 2017, **7**, 3924–3928.